

Supplementary Materials for

Enantioselective fragmentation of an achiral molecule in a strong laser field

K. Fehre*, S. Eckart, M. Kunitski, M. Pitzer, S. Zeller, C. Janke, D. Trabert, J. Rist, M. Weller, A. Hartung,
L. Ph. H. Schmidt, T. Jahnke, R. Berger, R. Dörner, M. S. Schöffler*

*Corresponding author. Email: fehre@atom.uni-frankfurt.de (K.F.); schoeffler@atom.uni-frankfurt.de (M.S.S.)

Published 8 March 2019, *Sci. Adv.* **5**, eaau7923 (2019)
DOI: 10.1126/sciadv.aau7923

This PDF file includes:

Notes to the *R/S* and *Re/Si* assignment

Dynamic chirality and the projection of the initial geometry to the final linear momenta by Coulomb explosion imaging

Estimation of the assignment error

Fig. S1. Simulation of the Coulomb explosion.

Fig. S2. The presentation of $\cos(\alpha)_{\text{initial-position}}$ as a function of $\cos(\alpha)$.

Fig. S3. Enantiomeric excess as a function of $\cos(\alpha)$.

References (33–36)

Notes to the *R/S* and *Re/Si* assignment

As to the *R/S* assignment of the molecular arrangements and the *Re/Si* assignment of the stereoheterotopic faces, we state here explicitly our convention as we are not aware that this case has been explicitly addressed in the CIP rules: For pyramidal arrangements, we took reference to the structure of the $n \rightarrow \pi^*$ excited state. We assumed the double bond of the carbonyl group to be broken and a stereogenic lone pair to be localised at the carbon atom. The latter receives the lowest priority of the four ligands, whereas the hydroxyl oxygen (O2) is given highest priority. This leads to the assignment of *R* to the structure in Fig. 2 A and *S* to the structure in Fig. 2 C. For the assignment of faces, we considered the electronic ground state situation and thus saturated the double bond of the carbonyl group as per the CIP prescription, which adds a ghost carbon atom (C) to the carbonyl oxygen and a ghost oxygen atom (O) to the carbonyl carbon atom. The latter is ignored, however, as suggested in Ref. (33) for prochiral molecules when establishing priorities. In the special case of the carboxylic acids (and for their Li or Be salts as well as possibly compounds with corresponding O-B bonds), this ghost C atom at the carbonyl oxygen gives priority to O1 over the singly bonded hydroxylic oxygen O2, such that finally in Fig. 1 the northern hemisphere (with $\cos(\theta) > 0$) belongs to the *Si* face of the prochiral formic acid.

Dynamic chirality and the projection of the initial geometry to the final linear momenta by Coulomb explosion imaging

Known as dynamic chirality (34), vibrational dynamics can bring achiral molecules transiently into a chiral shape. Any out of plane vibration, in particular the bending vibration of the H1 and the torsional vibration of the H2, lead to a chiral starting geometry for Coulomb explosion. These vibrations in the molecule merely lead to a widening of the distribution in $\cos(\alpha)$ around the equilibrium structure. For the planar ground state one expects a distribution around the value $\cos(\alpha) = 0$ and for a chiral equilibrium structure as known from the $n \rightarrow \pi^*$ excited state, one would expect a distribution with definite width around $\cos(\alpha) \approx 0.6$.

To illustrate this broadening and to verify how the transformation from the spatial molecular structure to the final linear momenta by the coulomb explosion remains unambiguous even for molecular structures bend out of the ground state structure (35), we performed classical simulations. Our simulation neglects the influence of the strong laser field and assumes the multiple ionization to be instantaneous. We allow the five instantaneous positively charged fragments to propagate from a given start position driven by their Coulomb repulsion. For a perfectly planar molecule, the final linear momenta lie in a plane. To estimate how bend start structures influence the final linear momenta, each atom is displaced from the equilibrium structure in the ground state in all three dimensions by a Gaussian distributed random value and the simulation is performed with this varied initial geometry (see fig. S1 A-C). This simulation shows that broader distributions in the initial geometry do not lead to systematic errors in the assignment of the fragments (fig. S1 D). Larger variations in the initial geometry (variance > 15 % of the C-H bond length) lead overlapping distributions in the final linear momenta, whereby the assignment of the fragments in the overlapping area is no longer unambiguous. However, this would lead to a loss of contrast in Fig. 1 rather than producing artificial effect. An estimation of the variation of the bond length due to vibration modes can be found in the literature (36) and ranges in the 10 % regime (for CO).

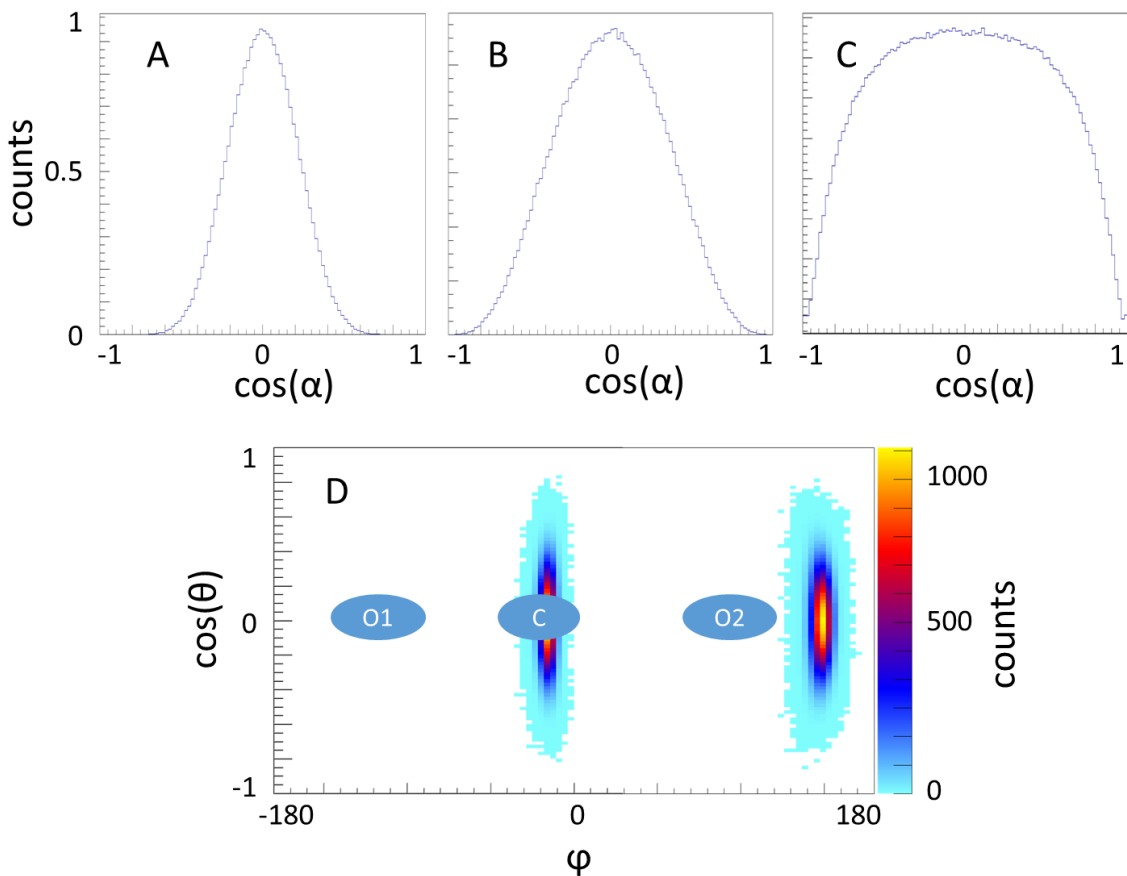


Fig. S1. Simulation of the Coulomb explosion. A, B and C show the symmetrical broadening of $\cos(\alpha)$ of the final momenta around the equilibrium structure for differently distributed initial spatial geometries. The variance of the start position of all fragments in X, Y and Z is in A 5.5% of the C-H (sp²-H) bond length of 108 pm, in B 8.3% and in C 18.4%. D The distributions of H1 and H2 in the molecular system shown for a variance in the starting distribution of 5.5% of the C-H bond length. The distribution around the C atom belongs to H1 and that near the O2 atom to H2. An increase in the variance leads to broader distributions in all final linear momenta, but not to an ambiguity in the assignment of the fragments beyond a overlapping of the distributions.

We would like to point out that the transformation from the initial spatial geometry of the molecule on the final linear momenta by the coulombic explosion is not linear. This is illustrated in fig. S2. Here, $\cos(\alpha)_{\text{initial-position}} = (\vec{r}_{O2} \times \vec{r}_{O1}) \cdot \vec{r}_{H1} / (|\vec{r}_{O2} \times \vec{r}_{O1}| \cdot |\vec{r}_{H1}|)$ the angle in the initial geometry- is plotted against $\cos(\alpha)$. As suggested by our data, in the initial spatial geometry H2 is bent by $\cos(-\alpha)_{\text{initial-position}}$ out of the molecular plane.

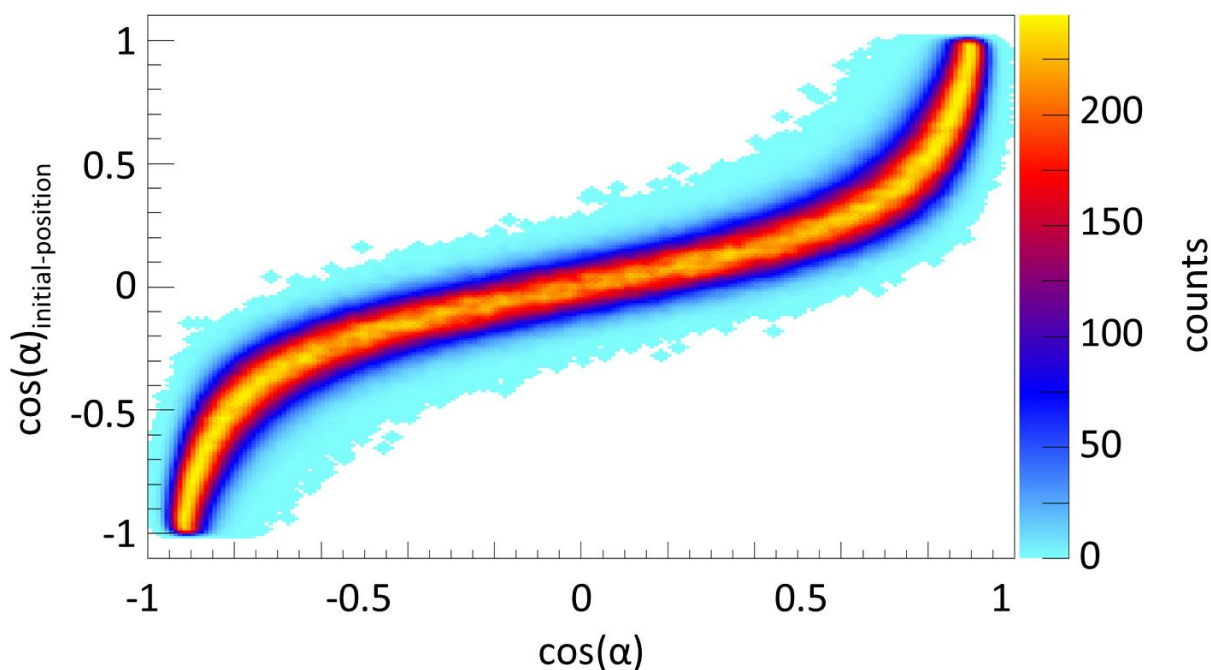


Fig. S2. The presentation of $\cos(\alpha)_{\text{initial-position}}$ as a function of $\cos(\alpha)$. The presentation of $\cos(\alpha)_{\text{initial-position}} = (\vec{r}_{02} \times \vec{r}_{01}) \cdot \vec{r}_{H1} / (|\vec{r}_{02} \times \vec{r}_{01}| |\vec{r}_{H1}|)$ as a function of $\cos(\alpha)$ (of final momenta) illustrates the nonlinearity of the projection from the initial spatial geometry to the final linear momenta by the coulomb explosion. To generate the initial distribution, first H1 and H2 were bent by the angle $\cos(\alpha)_{\text{initial-position}}$ out of the molecular plane, subsequently each atom was displaced from the bent structure in all three dimensions by a Gaussian distributed random value with a variance of 5.5% of the C-H bond length.

Estimation of the assignment error

In order to estimate the O assignment error, we examine the overlap region of the two structures in the negative X region in Fig. 4. By extrapolation, assuming a Gaussian distribution, the overlap area and thus the error-prone portion was estimated to be about 13%. For the determination of the H assignment error, we followed a different approach.

The maximum assignment error for the protons can be estimated directly from the distribution of $\cos(\alpha)$ in Fig 1a. The worst case would be that the assignment of the H atoms is random. This would lead to a symmetric distribution of $\cos(\alpha)$ around the value $\cos(\alpha) = 0$. Thus the actually observed enantiomeric excess (ee) in Fig 1A allows us to obtain a lower limit for the fraction of

events in which the proton assignment was correct. The enantiomeric excess is given by the normalized difference between the count rates $N_{\cos(\alpha)}$ for coincident detection of five singly charged atomic ions. This limit depends on $\cos(\alpha)$ and is shown in fig. S3. The considered molecular orientation was chosen to be $\cos(\theta) = 0.7$ and $\phi = 0^\circ$ where the influence of the helicity is small for all $\cos(\alpha)$ and the interchange of the two oxygen atoms does not affect the distribution in $\cos(\alpha)$.

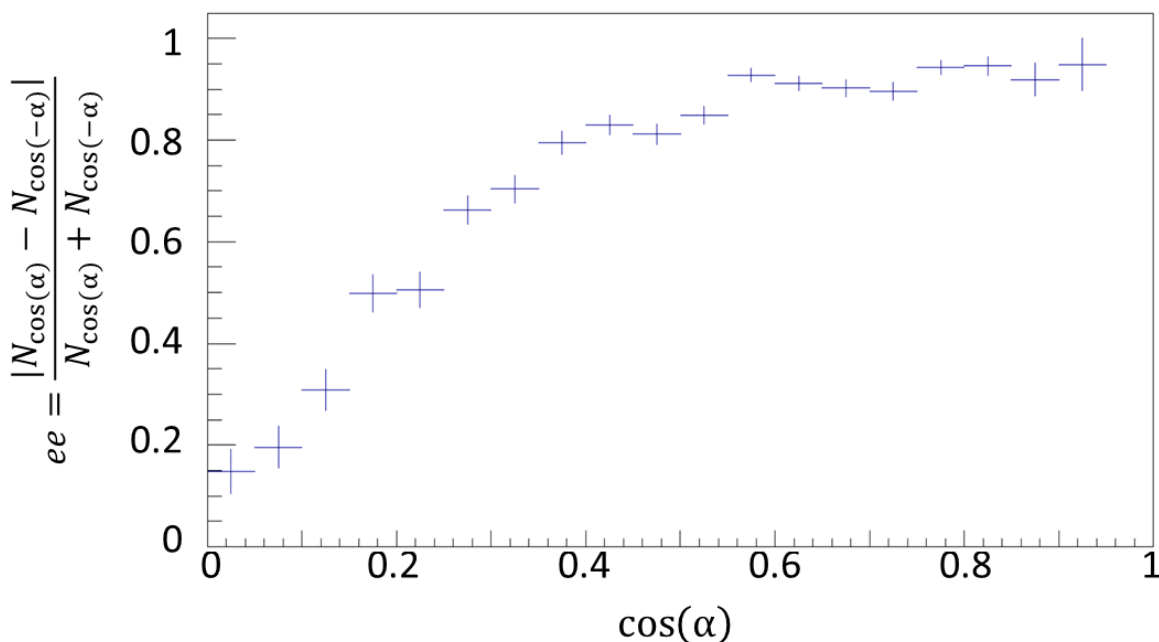


Fig. S3. Enantiomeric excess as a function of $\cos(\alpha)$. Enantiomeric excess (ee) as function of $\cos(\alpha)$ gating on $\cos(\theta) = 0.7$ and $\varphi = 0^\circ$. Since a wrong assignment of the protons leads to a sign change in $\cos(\alpha)$ while its absolute value remains conserved, the maximum value of the enantiomeric excess indicates the minimum proportion of correctly assigned protons. The dependency shown results from the actual ee for the different values of $\cos(\alpha)$, reduced by the proton assignment error.

Swapping the oxygen atoms in the triple product leads to a sign change in $\cos(\alpha)$ as well as interchanging the protons. Since the oxygen atoms are also included in the calculation for the orientation of the molecule, the error in the distribution of $\cos(\alpha)$ due to a wrong assignment of the oxygen atoms depends on the orientation of the molecule to the laser. The error in $\cos(\alpha)$ ranges between zero for a few selected orientations and approximately 8% for most of the other orientations. Thus, the proportion of molecules in which all fragments are correctly assigned is $0.93 * 0.87 = 0.81$. Due to this error, the observables (PICD and enantio-selectivity for different impact directions of light) appear smaller than they would be with 100 % correct assignment.